



Triphenylamine or carbazole-containing dibenzothiophene sulfones: Color-tunable solid-state fluorescence and hypso- or bathochromic mechanofluorochromic behaviors

Li-feng Yao^a, Xue-long Huang^b, Hong-ying Xia^a, Hai-feng He^{a,*}, Liang Shen^{a,**}

^a Jiangxi Engineering Laboratory of Waterborne Coating, School of Chemistry and Chemical Engineering, Jiangxi Science and Technology Normal University, Nanchang, 330013, People's Republic of China

^b College of Pharmacy, Gan Nan Medical University, Ganzhou, 341000, People's Republic of China

ARTICLE INFO

Keywords:

Triphenylamine
Carbazole
Dibenzothiophene sulfones
Highly emissive
Bathochromic mechanofluorochromic
Hypsochromic mechanofluorochromic

ABSTRACT

Four triphenylamine or carbazole-based highly emissive solid fluorophores (The maximum quantum yield of 42.43%) of dibenzothiophene sulfones have been successfully prepared and characterized. The solid-state emission behaviors and mechanical stimulus-responsive luminescence characteristics of all these donor-acceptor-donor (D-A-D) type or donor- π -acceptor- π -donor (D- π -A- π -D) type compounds 1–4 were investigated. Interestingly, these fluorophores 1–4 exhibited various solid-state fluorescent colors involving blue (CIE color coordinates of (0.15, 0.09)), blue-green (CIE color coordinates of (0.17, 0.43)), yellow (CIE color coordinates of (0.41, 0.56)) and brown-yellow (CIE color coordinates of (0.50, 0.50)). Furthermore, these dyes 1–4 also exhibited different mechanofluorochromic behaviors. More specifically, luminogens 1–3 showed bathochromic mechanofluorochromic phenomena. However, luminogen 4 showed distinct-different hypsochromic mechanofluorochromic phenomenon. All these observed mechanochromic emission conversions could be repeated for many cycles. Single-crystal X-ray diffraction and powder X-ray diffraction experiments demonstrated that the mechanofluorochromic behaviors of 1–4 were related to the morphology transformation from crystalline state to amorphous state.

1. Introduction

Mechanofluorochromism is an interesting phenomenon of fluorescent color change resulted from mechanical stimulus of a solid sample [1–6]. For more than a decade, mechanofluorochromic fluorophores have received much attention on account of their potential applications in the fabrication of optical-data storage devices and fluorescent sensors [7–15]. Meanwhile, the development of highly solid-state emissive organic dyes is also a topic of current interest owing to their possible applications in organic light-emitting diodes (OLED) and luminescent displays [16–28]. Furthermore, bright solid-state emission is a rather important factor for the preparation of high-contrast mechanochromic fluorescence materials [29–41]. However, numerous fluorescent compounds show faint fluorescence or non-fluorescence in the solid state because of the thorny aggregation-caused quenching (ACQ) phenomenon [42]. Indeed, it is well-known that the excited states of compounds

possessing ACQ effect often decay via non-radiative pathways upon aggregation. Fortunately, an important aggregation-induced emission (AIE) effect, which is precisely the inverse of ACQ, was firstly reported by Tang's group [43]. Admittedly, the discovery of AIE phenomenon provides an important step forward to expand the number of highly solid-state emissive mechanofluorochromic materials [44–46]. In general, bright solid-state fluorescence of AIE-active compounds is usually caused by the restriction of their intramolecular rotations [47]. Therefore, the twisted molecular conformation of triphenylamine or carbazole fluorogen is conducive to the construction of highly efficient emission materials [48–55]. On the other hand, π -conjugated fluorescent molecules with donor and acceptor moieties are promising candidates for functional luminescent materials, and the emission properties of many solid materials with donor-acceptor (D-A) groups are sensitive to external stimuli. In fact, during the last decade, a lot of D-A type organic fluorophores with stimuli-responsive properties have been reported

* Corresponding author.

** Corresponding author.

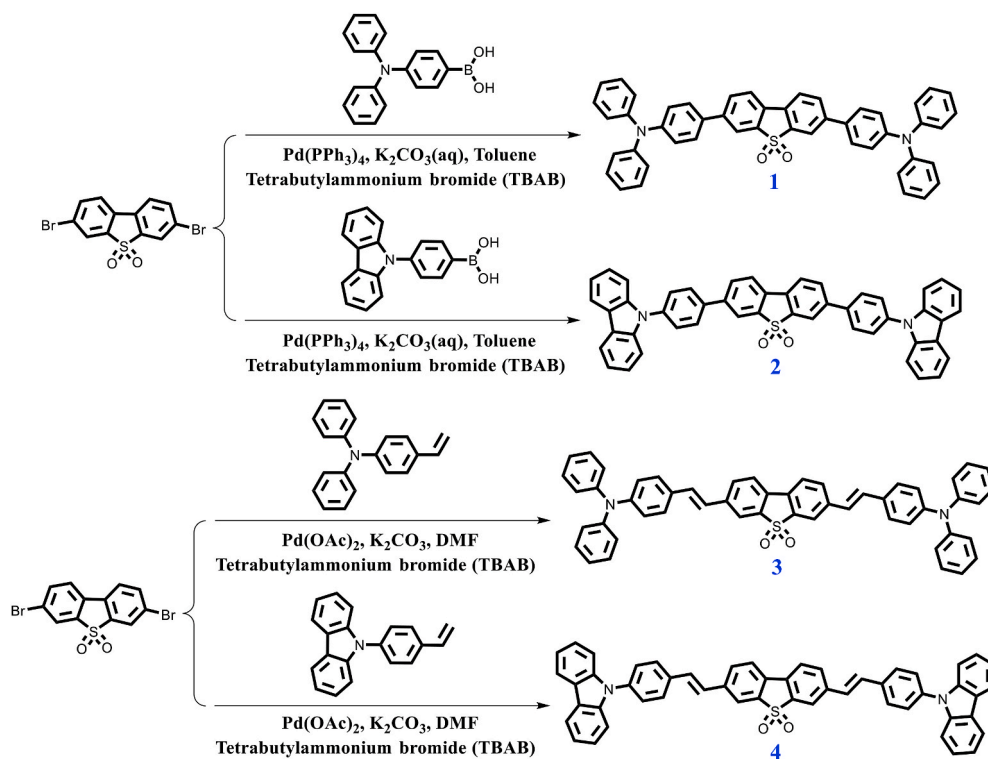
E-mail addresses: hehf0427@jxstnu.com.cn (H.-f. He), liangshen@jxstnu.com.cn (L. Shen).

<https://doi.org/10.1016/j.dyepig.2020.108747>

Received 9 May 2020; Received in revised form 4 July 2020; Accepted 4 July 2020

Available online 29 August 2020

0143-7208/© 2020 Elsevier Ltd. All rights reserved.



Scheme 1. Synthesis of the compounds 1, 2, 3 and 4.

[56–58]. Luminescent properties of solid organic dyes are closely associated with their molecular packing modes, and a variety of compounds with different light-emitting wavelengths can be obtained conveniently via rational molecular design. However, it is still a great challenge to realize nearly full-color emission based on the same donor and acceptor units. Incorporation of two electron-donating moieties containing rotatable aromatic rings into the strongly electron-withdrawing framework may be a rational design strategy. More importantly, by simply changing the electron-donating units and modulating the length of π -conjugated skeletons, the related solid-state emission colors can be effectively regulated, and external mechanical stimulation can further tune the solid-state fluorescence (see Scheme 1).

To date, numerous organic and organometallic compounds exhibiting mechanochromic luminescence behavior have been discovered, and the majority of these reported mechanochromic luminogens show bathochromic emission spectral changes after grinding. In contrast, luminophors with hypsochromic mechanochromic behavior are still extremely rare. Furthermore, it is very difficult to obtain a series of similarly structural compounds with hypso- and bathochromic mechanofluorochromic phenomena simultaneously basing on the same core units. In this study, we attempted to introduce two electron-donating triphenylamine or carbazole fluorogens into one electron-withdrawing dibenzothiophene sulfone moiety. Consequently, four D-A-D type or D- π -A- π -D type compounds 1–4 were successfully obtained. Interestingly, luminogens 1–4 showed high-intensity solid-state fluorescence with various colors containing blue, blue-green, yellow and brown-yellow. More excitingly, 1–4 also showed reversible and hypso- or bathochromic mechanofluorochromic characteristics.

2. Materials and methods

2.1. Experimental

General: The starting materials 3,7-dibromodibenzo [b,d]thiophene 5,5-dioxide, 4-(diphenylamino)phenylboronic acid and 4-(9H-carbazol-9-yl) phenylboronic acid purchased from J&K Chemical were used as

received. All other starting materials and all reagents were obtained via commercial suppliers and then applied without further purification. All experimental manipulations were carried out under an argon atmosphere by using standard Schlenk techniques. ^1H NMR (400 MHz) and ^{13}C NMR (100.6 MHz) spectra were collected on American Varian Mercury Plus 400 spectrometer (400 MHz). ^1H NMR spectra are reported as followed: chemical shift in ppm (δ) relative to the chemical shift of TMS at 0.00 ppm, integration, multiplicities (s = singlet, d = doublet, t = triplet and m = multiplet), and coupling constant (Hz). ^{13}C NMR chemical shifts reported in ppm (δ) relative to the central line of triplet for CDCl_3 at 77 ppm. Mass spectral data were recorded on a Bruker UltrafleXtreme MALDI-TOF-TOF mass spectrometer. Elemental analyses (C, H, N) were carried out with a PE CHN 2400 analyzer. Fluorescence spectra were recorded by fluorescence spectrometer (FLS980, Edinburgh Instruments). The absolute fluorescence quantum yields were measured by HAMAMATSU ABSOLUTE PL QUANTUM YIELD SPECTROMETER C11347. The fluorescence lifetimes were measured by FLS980. XRD studies of compounds 1–4 were recorded on a Shimadzu XRD-6000 diffractometer (Japan) ($\text{Cu K}\alpha$, 40 kV and 30 mA). X-ray crystal structures of compounds 1 and 2 were obtained on a Bruker APEX DUO CCD system (Germany), and their structures were fully analyzed by a combination of direct methods (SHELXS-97) and fourier difference techniques and refined by full-matrix least-squares (SHELXL-97), and their crystallographic data of compounds 1 and 2 were deposited in the Cambridge Crystallographic Data Centre as supplemental publication CCDC 2002533 (compound 1) and CCDC 2002534 (compound 2). Column chromatographic separations of the target compounds 1–4 were carried out on silica gel (200–300 mesh).

2.2. Synthesis

2.2.1. General procedure for the synthesis of compound 1

A mixture of 3,7-dibromodibenzo [b,d]thiophene 5,5-dioxide (1.12 g, 3.01 mmol), (4-(diphenylamino)phenyl)boronic acid (1.88 g, 6.50 mmol), K_2CO_3 (2 mol/L, 5 ml, aqueous solution), TBAB (0.71 g, 2.21 mmol), $\text{Pd}(\text{PPh}_3)_4$ (0.35 g, 0.30 mmol) were stirred in toluene (60 ml)

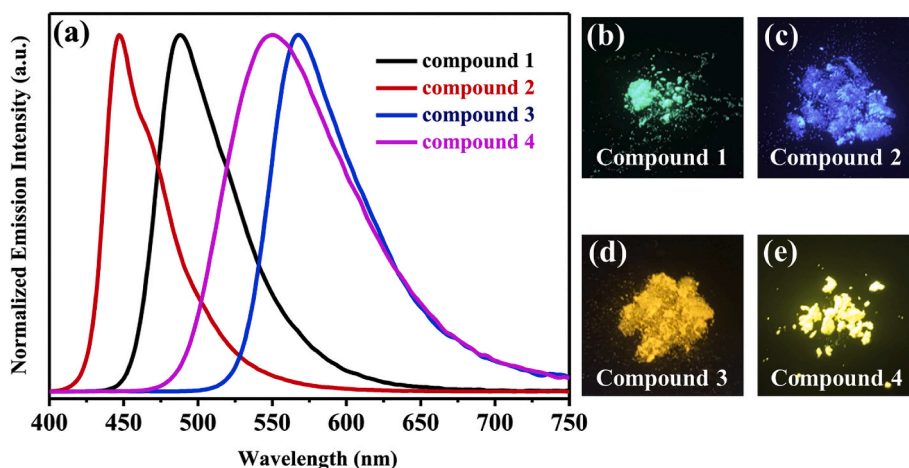


Fig. 1. (a) Solid-state emissive spectra of the compounds 1, 2, 3 and 4. The related solid-state fluorescence images under 365 nm UV light: (b): compound 1; (c): compound 2; (d): compound 3; (e): compound 4.

for 24 h under an argon atmosphere at 80 °C, after completion of present reaction, the mixture was extracted with dichloromethane (3 × 70 mL), the combined organic layers were washed with brine, dried (MgSO₄), and concentrated in vacuo. The residues were purified by column chromatography, affording the yellow solid product in a yield of 73.2%. **1:** ¹H NMR (400 MHz, CDCl₃): δ (ppm) = 7.93 (s, 2H), 7.73 (s, 4H), 7.42 (d, *J* = 8 Hz, 4H), 7.24–7.18 (m, 8H), 7.08 (d, *J* = 8 Hz, 12H), 7.01 (t, *J* = 6 Hz, 4H). ¹³C NMR (100.6 MHz, CDCl₃): δ (ppm) = 148.47, 147.33, 143.00, 138.74, 132.00, 131.71, 129.61, 129.42, 127.64, 124.93, 123.53, 123.16, 121.77, 119.91. ESI-MS: *m/z* = 703.2 [M]⁺. Anal. Calcd. for C₄₈H₃₄N₂O₂S: C, 82.02; H, 4.88; N, 3.99. Found: C, 82.11; H, 4.96; N, 3.93.

2.2.2. General procedure for the synthesis of compound 2

A mixture of 3,7-dibromodibenzo [b,d]thiophene 5,5-dioxide (1.12 g, 3.01 mmol), (4-(9H-carbazol-9-yl)phenyl)boronic acid (1.88 g, 6.55 mmol), K₂CO₃ (2 mol/L, 5 ml, aqueous solution), TBAB (0.71 g, 2.21 mmol), Pd(PPh₃)₄ (0.35 g, 0.30 mmol) were stirred in toluene (60 ml) for 24 h under an argon atmosphere at 80 °C, after completion of present reaction, the mixture was extracted with dichloromethane (3 × 70 mL), the combined organic layers were washed with brine, dried (MgSO₄), and concentrated in vacuo. The residues were purified by column chromatography, affording the white solid product in a yield of 71.8%. **2:** ¹H NMR (400 MHz, CDCl₃): δ (ppm) = 8.11 (d, *J* = 4 Hz, 6H), 7.94–7.89 (m, 4H), 7.82 (d, *J* = 8 Hz, 4H), 7.66 (d, *J* = 8 Hz, 4H), 7.44–7.37 (m, 8H), 7.28 (s, 1H), 7.24 (s, 1H), 7.19 (s, 2H). ¹³C NMR (100.6 MHz, CDCl₃): δ (ppm) = 142.89, 140.70, 139.09, 138.32, 137.69, 132.57, 130.41, 128.51, 127.65, 126.11, 123.64, 122.21, 120.78, 120.42, 120.27, 109.76. ESI-MS: *m/z* = 699.2 [M]⁺. Anal. Calcd. for C₄₈H₃₀N₂O₂S: C, 82.50; H, 4.33; N, 4.01. Found: C, 82.55; H, 4.39; N, 3.94.

2.2.3. General procedure for the synthesis of compound 3

A mixture of 3,7-dibromodibenzo [b,d]thiophene 5,5-dioxide (1.12 g, 3.01 mmol), N,N-diphenyl-4-vinylaniline (4.08 g, 15.05 mmol), Pd(OAc)₂ (26.87 mg, 0.12 mmol), K₂CO₃ (1.08 g, 7.83 mmol), and TBAB (2.03 g, 6.32 mmol) in anhydrous DMF (60 ml) was reacted under argon atmosphere at 110 °C for 24 h, after completion of present reaction, the mixture was extracted with dichloromethane (3 × 70 mL), the combined organic layers were washed with brine, dried (MgSO₄), and concentrated in vacuo. The residues were purified by column chromatography, affording the orange solid product in a yield of 61.2%. **3:** ¹H NMR (400 MHz, CDCl₃): 7.84 (s, 2H), 7.58–7.52 (m, 4H), 7.30 (d, *J* = 8 Hz, 4H), 7.20 (t, *J* = 8 Hz, 8H), 7.08–6.96 (m, 18H), 6.88 (d, *J* = 16 Hz, 2H). ¹³C NMR (100.6 MHz, CDCl₃): δ (ppm) = 148.25, 147.34, 140.16, 138.60,

131.69, 131.08, 130.14, 129.79, 129.37, 127.80, 124.86, 124.35, 123.43, 122.95, 121.60, 118.99. ESI-MS: *m/z* = 755.2 [M]⁺. Anal. Calcd. for C₅₂H₃₈N₂O₂S: C, 82.73; H, 5.07; N, 3.71. Found: C, 82.65; H, 5.01; N, 3.80.

2.2.4. General procedure for the synthesis of compound 4

A mixture of 3,7-dibromodibenzo [b,d]thiophene 5,5-dioxide (1.12 g, 3.01 mmol), 9-(4-vinylphenyl)-9H-carbazole (4.05 g, 15.05 mmol), Pd(OAc)₂ (26.87 mg, 0.12 mmol), K₂CO₃ (1.08 g, 7.83 mmol), and TBAB (2.03 g, 6.32 mmol) in anhydrous DMF (60 ml) was reacted under argon atmosphere at 110 °C for 24 h, after completion of present reaction, the mixture was extracted with dichloromethane (3 × 70 mL), the combined organic layers were washed with brine, dried (MgSO₄), and concentrated in vacuo. The residues were purified by column chromatography, affording the yellow solid product in a yield of 60.5%. **4:** The NMR data of the compound were not obtained due to the poor solubility. ESI-MS: *m/z* = 751.2 [M]⁺. Anal. Calcd. for C₅₂H₃₄N₂O₂S: C, 83.17; H, 4.56; N, 3.73. Found: C, 83.10; H, 4.61; N, 3.65.

3. Results and discussion

3.1. Design and synthesis of target molecules 1–4

As a strong electron-withdrawing group, dibenzothiophene sulfone has been widely used to construct photoelectric functional materials [59,60]. Furthermore, the electron-donating triphenylamine or carbazole group has also been extensively applied in the field of fluorescent materials [61]. Therefore, in this work, we linked two triphenylamine or carbazole groups to one dibenzothiophene sulfone moiety via the typical Suzuki coupling reaction or Heck coupling reaction. As a result, four target compounds 1–4 were successfully synthesized. Compounds 1 and 2 belong to D-A-D type fluorescent molecules, and compounds 3 and 4 belong to D-π-A-π-D type fluorescent molecules.

3.2. Solid-state emission and solvatochromic fluorescence behaviors of compounds 1–4

To investigate the solid-state emission properties of D-A-D type compounds 1 and 2 or D-π-A-π-D type compounds 3 and 4 in detail, their corresponding solid-state photoluminescence (PL) spectra were obtained, and the fluorescence properties of all the compounds in the solid state are shown in Fig. 1. Obviously, the solid-state fluorescent colors of 1–4 presented a considerable change. The PL spectrum of triphenylamine-based D-A-D type fluorescent dye 1 exhibited one emission band with a λ_{max} at 488 nm. Furthermore, the solid powder 1

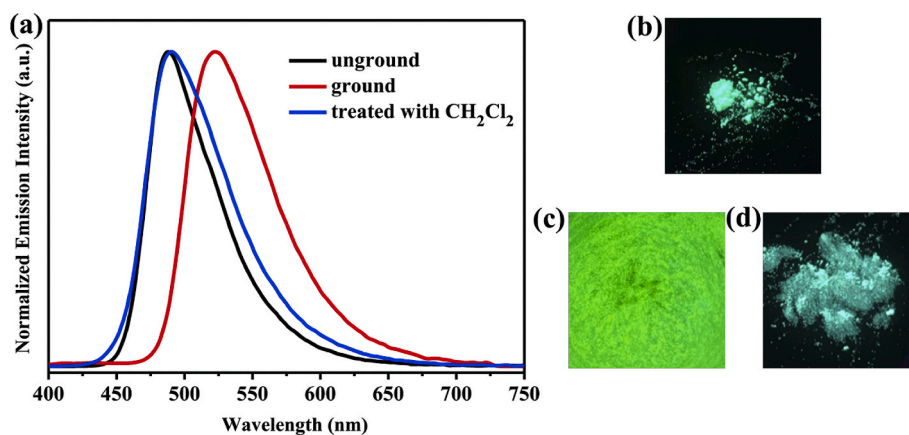


Fig. 2. (a) Solid-state emissive spectra of solid sample 1 at different conditions. Excitation wavelength: 365 nm. (b) Fluorescence image of the unground sample 1 under 365 nm UV light. (c) Fluorescence image of the ground sample 1 under 365 nm UV light. (d) Fluorescence image of the ground sample 1 after treatment with dichloromethane under 365 nm UV light.

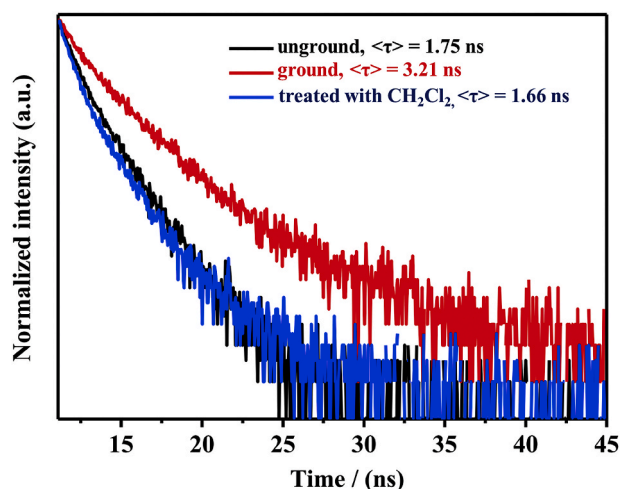


Fig. 3. Fluorescence decay curves of unground solid sample 1 (488 nm), ground solid sample 1 (523 nm), ground solid sample 1 (490 nm) after treatment with dichloromethane.

emitted strong blue-green fluorescence, and its fluorescence quantum yield was 12.35%. By changing the electron-donating aromatic group substituent, the emission wavelength of solid-state fluorescent dye 2 presented a blue-shift from 488 to 447 nm, and the solid powder 2 emitted strong blue fluorescence with the quantum yield of 10.05%. By extending the degree of π -conjugation, the solid-state fluorescence spectrum of D- π -A- π -D type fluorescent dye 3 exhibited one emission band with a λ_{max} at 568 nm, and the fluorescent dye exhibited strong brown-yellow luminescence with the quantum yield of 10.96%. Similarly, by changing the electron-donating aromatic group substituent, the emission wavelength of solid-state fluorescent dye 4 also presented a blue-shift from 568 to 550 nm, and the solid powder 4 also exhibited strong yellow fluorescence with high quantum yield of 42.43%. Moreover, solid-state compounds 1–4 showed good thermal stability with high onset degradation temperatures (T_d) ranging from 350 to 430 °C (Supporting information: Fig. S1). In addition, compound 1, 2, 3 or 4 in pure toluene (1.0×10^{-5} mol L $^{-1}$) exhibited one emission band with a λ_{max} at 460 nm, 426 nm, 498 nm and 450 nm, respectively. Interestingly, the maximum emission wavelength of 1, 2, 3 or 4 in various solvents red-shifted gradually with increasing solvent polarity, and thus compounds 1–4 showed outstanding solvatochromic fluorescence characteristics (Supporting information: Fig. S2). Furthermore, the aggregation-induced fluorescence behaviors of compounds 1–4 were

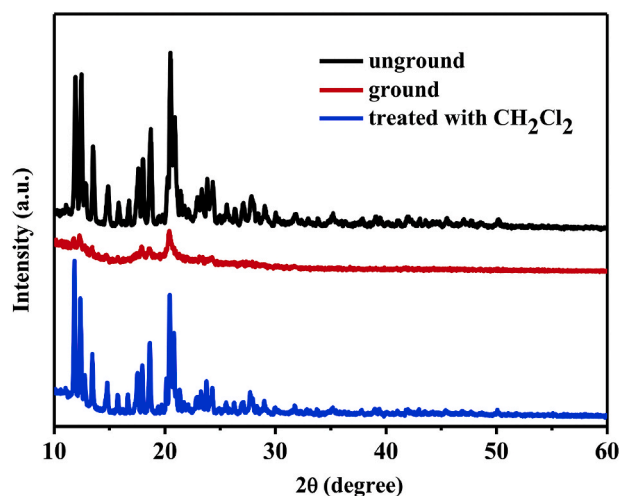


Fig. 4. Powder XRD patterns of compound 1 in different solid states.

also studied, and the obvious aggregate fluorescence change phenomena of 1–4 are observed (Supporting information: Fig. S3). Clearly, compounds 1–4 exhibited green fluorescence, cyan fluorescence, brown-yellow fluorescence and yellow fluorescence in DMF-water mixture (water fraction: 90%), respectively. These results were consistent with the different solid-state fluorescence properties of 1–4.

3.3. The bathochromic mechanofluorochromic phenomena of D-A-D type compounds 1 and 2

As mentioned above, the pristine solid sample of compound 1 emitted blue-green fluorescence with the average lifetime of 1.75 ns (Fig. 3). As can be seen in Fig. 2, through grinding the solid sample with a pestle in a mortar, an emission band with a λ_{max} at 523 nm appeared, and the ground powder emitted clear green fluorescence with the average lifetime of 3.21 ns (Fig. 3). Furthermore, when the ground powder was fumed with vapor of dichloromethane for 1 min, the fluorescence color rapidly reverted to blue-green, and the average lifetime decreased to 1.66 ns (Fig. 3). Therefore, the mechanofluorochromic phenomenon of compound 1 was reversible.

Subsequently, the powder X-ray diffraction (PXRD) patterns were investigated to determine the mechanofluorochromic mechanism of 1 (Fig. 4), a number of sharp diffraction peaks of the pristine solid powder of 1 were seen in its XRD pattern, suggesting that the unground sample 1

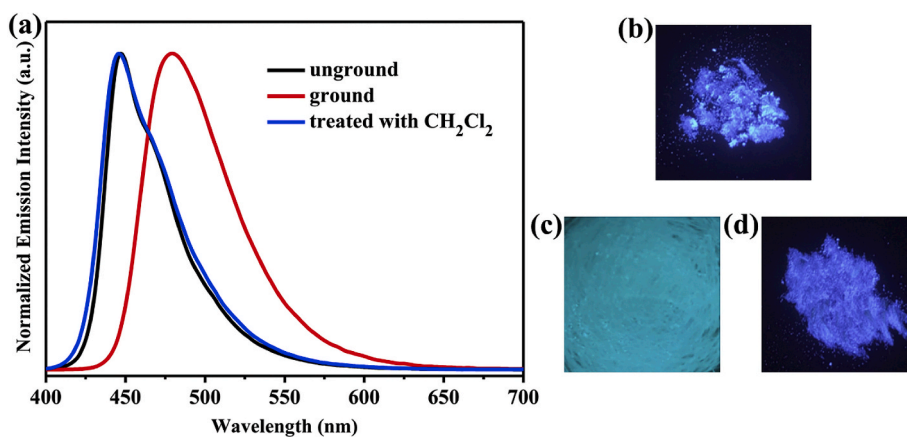


Fig. 5. (a) Solid-state emissive spectra of solid sample 2 at different conditions. Excitation wavelength: 365 nm. (b) Fluorescence image of the unground sample 2 under 365 nm UV light. (c) Fluorescence image of the ground sample 2 under 365 nm UV light. (d) Fluorescence image of the ground sample 2 after treatment with dichloromethane under 365 nm UV light.

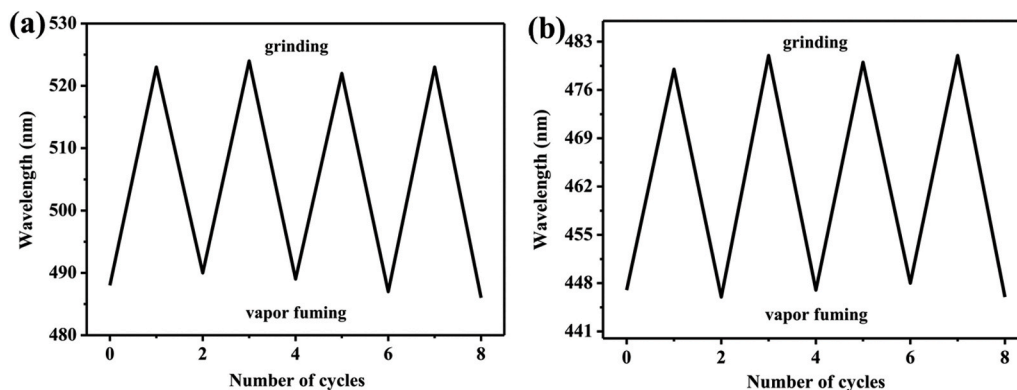


Fig. 6. (a) Repetitive experiment of mechanofluorochromic effect for 1. (b) Repetitive experiment of mechanofluorochromic effect for 2.

was crystalline in nature. After grinding, many diffraction peaks disappeared and several diffraction peaks weakened. This XRD result revealed that the ground sample 1 was amorphous in nature. Moreover, the treated sample exhibited strong diffraction peaks again, which were almost the same as those for the unground sample, when the ground powder was exposed to dichloromethane vapor for 1 min. This phenomenon indicated the recovery of the crystalline nature. Clearly, the reversible mechanofluorochromic process could be attributed to the reversible phase transition between the stable crystalline phase and the metastable amorphous phase. Similarly, compound 2 also exhibited reversible mechanochromic fluorescence phenomenon with the color transformation from blue to blue-green and vice versa (Fig. 5). When solid sample 2 was ground, it was possible that structural organization of 2 became more planarity, and thus luminogen 2 showed mechanochromic phenomenon involving red-shifted fluorescent color transformation. The patterns of powder XRD also confirmed that the transformation between crystalline and amorphous states was responsible for the mechanofluorochromic mechanism of 2 (Supporting information: Fig. S5). Moreover, as shown in Fig. 6, the mechanofluorochromic behavior of D-A-D type dye 1 or 2 could be repeated four times without obvious changes. Therefore, the reversibility of mechanofluorochromic phenomenon of fluorescent molecule 1 or 2 is excellent.

To get deep understanding of the mechanofluorochromic mechanism of compound 1 or 2, single crystals of 1 and 2 were obtained by tardily diffusing n-hexane vapor into their dichloromethane solutions, and their single-crystal structures were also resolved. As can be seen in Fig. 7 and Fig. 8, in the crystals of 1 and 2, molecules 1 and 2 are packed through

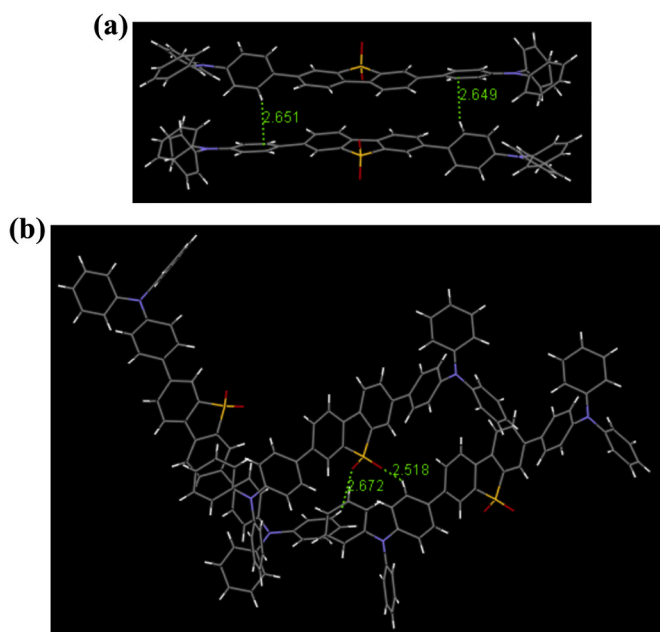


Fig. 7. (a) Crystal packing structure of compound 1. Showing C-H ... π interactions (2.651 Å and 2.649 Å). (b) Crystal packing structure of compound 1. Showing C-H...O interactions (2.672 Å and 2.518 Å).

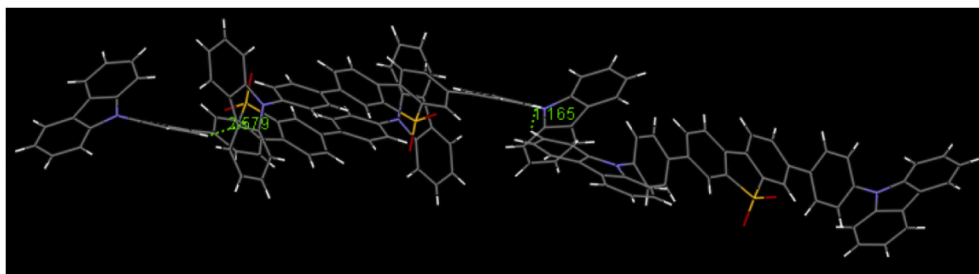


Fig. 8. Crystal packing structure of compound 2. Showing C–H ... π interactions (1.165 Å and 2.579 Å).

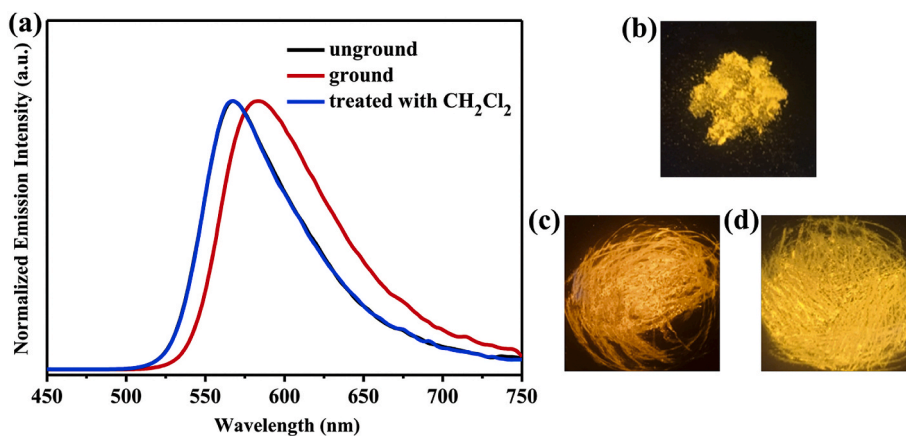


Fig. 9. (a) Solid-state emissive spectra of solid sample 3 at different conditions. Excitation wavelength: 365 nm. (b) Fluorescence image of the unground sample 3 under 365 nm UV light. (c) Fluorescence image of the ground sample 3 under 365 nm UV light. (d) Fluorescence image of the ground sample 3 after treatment with dichloromethane under 365 nm UV light.

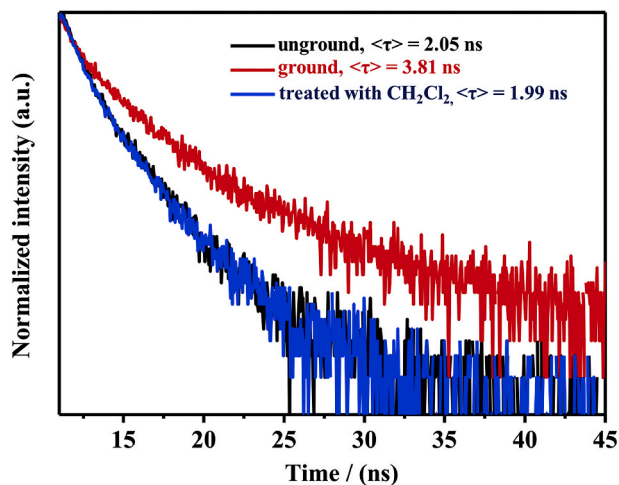


Fig. 10. Fluorescence decay curves of unground solid sample 3 (568 nm), ground solid sample 3 (584 nm), ground solid sample 3 (567 nm) after treatment with dichloromethane.

weak C–H ... π interactions (2.651 Å and 2.649 Å for 1, 1.165 Å and 2.579 Å for 2) and C–H...O interactions (2.672 Å and 2.518 Å for 1). Furthermore, no intermolecular π ... π interactions are observed in the crystals of 1 and 2, and the highly twisted molecular conformations of 1 and 2 are beneficial to the realization of strong solid-state fluorescence. When the solid samples 1 and 2 were ground, their molecular packings were changed, which affected the intramolecular charge transfer characters of molecules 1 and 2. As a consequence, their solid-state fluorescence could be adjusted by mechanical force.

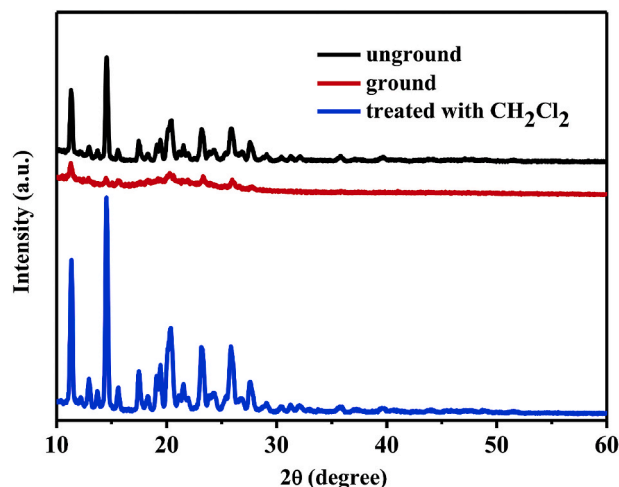


Fig. 11. Powder XRD patterns of compound 3 in different solid states.

3.4. The bathochromic and hypsochromic mechanofluorochromic phenomena of *D*- π -A- π -D type compounds 3 and 4

As shown in Fig. 9, the as-prepared sample 3 exhibited a broad brown-yellow emission peak at 568 nm, and the average lifetime of the pristine solid possessing brown-yellow fluorescence was 2.05 ns (Fig. 10). It was notable that mechanical grinding caused a red-shift of the emission to 584 nm, and a powder with the average lifetime of 3.81 ns (Fig. 10) that emitted orange fluorescence was obtained. Furthermore, the initial brown-yellow fluorescence could be recovered upon treatment of the ground sample 3 with fuming dichloromethane for 1

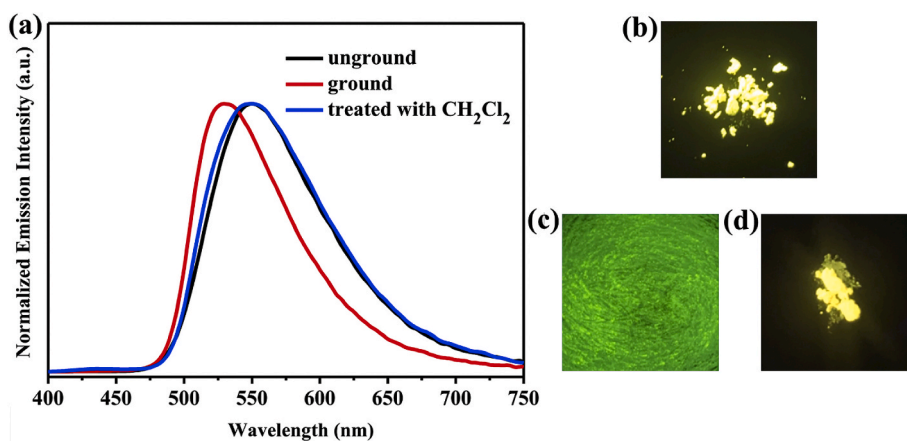


Fig. 12. (a) Solid-state emissive spectra of solid sample 4 at different conditions. Excitation wavelength: 365 nm. (b) Fluorescence image of the unground sample 4 under 365 nm UV light. (c) Fluorescence image of the ground sample 4 under 365 nm UV light. (d) Fluorescence image of the ground sample 4 after treatment with dichloromethane under 365 nm UV light.

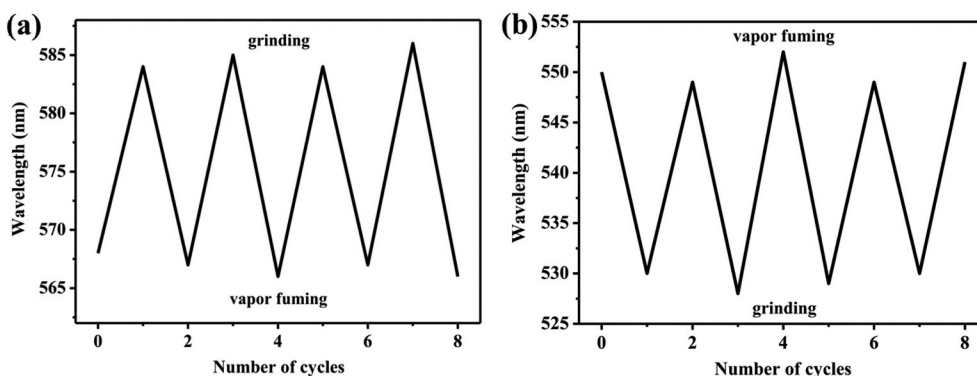


Fig. 13. (a) Repetitive experiment of mechanofluorochromic effect for 3. (b) Repetitive experiment of mechanofluorochromic effect for 4.

min. Meanwhile, the corresponding average lifetime also decreased to 1.99 ns (Fig. 10), which was close to that of the as-prepared solid sample. Therefore, D- π -A- π -D type dye 3 exhibited reversible bathochromic mechanofluorochromism behavior. It is conjectured that the structural packing of compound 3 becomes more planarity upon grinding.

Subsequently, the PXRD measurements were carried out to study the underlying origin of the mechanofluorochromic behavior of 3 (Fig. 11), and the PXRD patterns demonstrated that the as-synthesized samples and vapor-fumed samples had nearly identical strong diffraction peaks, indicating the crystalline feature of as-prepared solid powder 3 and sample 3 after dichloromethane treatment. Furthermore, the measurement result also revealed that vapor treatment could induce the recovery of the initial crystalline state. However, the XRD pattern of the ground solids of 3 became broad and weak, and many sharp diffraction peaks disappeared, suggesting the amorphous nature of ground sample 3. As a result, the bathochromic emission was possibly related to the collapse of crystalline lattice of 3 during grinding.

Interestingly, carbazole-based D- π -A- π -D type compound 4 exhibited hypsochromic mechanofluorochromic phenomenon involving color transformation from yellow to green (Fig. 12), and this fluorescent color change process was reversible upon treatment of the ground sample with fuming dichloromethane for 1 min. It is possible that the planarity of structural packing of compound 4 after grinding becomes worse. From the PXRD results (Supporting information: Fig. S7), the hypsochromic mechanochromic fluorescence phenomenon of 4 could also be attributed to the interconversion between crystalline and amorphous phases. In addition, the fluorescence-variation process of D- π -A- π -D type dye 3

or 4 could be repeated many times (Fig. 13), indicating the superior reversibility. The maximum emission wavelengths of compounds 1–4 in different solid states were summarized in a table (Supporting information: Fig. S8).

4. Conclusions

In conclusion, four dibenzothiophene sulfone-based solid fluorophores have been designed and synthesized. Among them, compounds 1 and 2 belong to D-A-D type structure, and compounds 3 and 4 belong to D- π -A- π -D type structure, in which the two triphenylamine or carbazole groups are electron donors and the dibenzothiophene sulfone acts as an electron-accepting unit. Interestingly, these luminogens show highly solid-state emissive behaviors with different fluorescent colors involving blue, blue-green, yellow and brown-yellow. Furthermore, these dyes 1–4 also show reversible and hypso- or bathochromic mechanofluorochromic phenomena. More specifically, 1–3 show bathochromic mechanofluorochromic characteristics. However, luminogen 4 shows distinct-different hypsochromic mechanofluorochromic behavior. This work will be valuable for designing excellent candidate mechanofluorochromic materials with full-color emission.

Author statement

Li-feng Yao: Investigation.
Xue-long Huang: Investigation.
Hong-ying Xia: Supervision.
Hai-feng He: Supervision, Writing.

Liang Shen: Supervision.

Declaration of competing interest

The authors declare that they have no known competing financial interests or personal relationships that could have appeared to influence the work reported in this paper.

Acknowledgments

The authors are grateful for the financial support from the National Natural Science Foundation of China (21867011, 51563011); Natural Science Foundation of Jiangxi Province (20192BAB213008).

Appendix A. Supplementary data

Supplementary data to this article can be found online at <https://doi.org/10.1016/j.dyepig.2020.108747>.

References

- Chen Y, Zhang X, Wang M, Peng J, Zhou Y, Huang X, et al. Mechanofluorochromism, polymorphism and thermochromism of novel D- π -A piperidin-1-yl-substituted isoquinoline derivatives. *J Mater Chem C* 2019;7: 12580–7.
- Gon M, Kato K, Tanaka K, Chujo Y. Elastic and mechanofluorochromic hybrid films with POSS-capped polyurethane and polyfluorene. *Mater Chem Front* 2019;3: 1174–80.
- Chen Z, Li Z, Hu F, Yu GA, Yin J, Liu SH. Novel carbazole-based aggregation-induced emission-active gold(I) complexes with various mechanofluorochromic behaviors. *Dyes Pigments* 2016;125:169–78.
- Xu P, Qiu Q, Ye X, Wei M, Xi W, Feng H, et al. Halogenated tetraphenylethene with enhanced aggregation-induced emission: an anomalous anti-heavy-atom effect and self-reversible mechanochromism. *Chem Commun* 2019;55:14938–41.
- Xu D, Wang Y, Li L, Zhou H, Liu X. Aggregation-induced enhanced emission-type cruciform luminophore constructed by carbazole exhibiting mechanical force-induced luminescence enhancement and chromism. *RSC Adv* 2020;10:12025–34.
- Chen Z, Tang JH, Chen W, Xu Y, Wang H, Zhang Z, et al. Temperature- and mechanical-force-responsive self-assembled rhomboidal metallacycle. *Organometallics* 2019;38:4244–9.
- Lee GH, Han SH, Kim JB, Kim JH, Lee JM, Kim SH. Colloidal photonic inks for mechanochromic films and patterns with structural colors of high saturation. *Chem Mater* 2019;31:8154–62.
- Chen Z, Zhang J, Song M, Yin J, Yu GA, Liu SH. A novel fluorene-based aggregation-induced emission (AIE)-active gold(I) complex with crystallization-induced emission enhancement (CIEE) and reversible mechanochromism characteristics. *Chem Commun* 2015;51:326–9.
- Zhao J, Chi Z, Zhang Y, Mao Z, Yang Z, Ubba E, et al. Recent progress in the mechanofluorochromism of cyanoethylene derivatives with aggregation-induced emission. *J Mater Chem C* 2018;6:6327–53.
- Crenshaw BR, Burnworth M, Khariwala D, Hiltner A, Mather PT, Simha R, et al. Deformation-induced color changes in mechanochromic polyethylene blends. *Macromolecules* 2007;40:2400–8.
- Yin Y, Chen Z, Fan C, Liu G, Pu S. 1,8-Naphthalimide-based highly emissive luminophors with various mechanofluorochromism and aggregation-induced characteristics. *ACS Omega* 2019;4:14324–32.
- Zhang T, Han Y, Liang M, Bian W, Zhang Y, Li X, et al. Substituent effect on photophysical properties, crystal structures and mechanochromism of D- π -A phenothiazine derivatives. *Dyes Pigments* 2019;171:107692.
- Wang Y, Li M, Zhang Y, Yang J, Zhu S, Sheng L, et al. Stress acidulated amphoteric molecules and mechanochromism via reversible intermolecular proton transfer. *Chem Commun* 2013;49:6587–9.
- Gundu S, Kim M, Mergu N, Son YA. AIE-active and reversible mechanochromic tetraphenylethene-tetradiphenylacrylonitrile hybrid luminogens with re-writable optical data storage application. *Dyes Pigments* 2017;146:7–13.
- Cho S, Kang S, Pandya A, Shanker R, Khan Z, Lee Y, et al. Large-area cross-aligned silver nanowire electrodes for flexible, transparent, and force-sensitive mechanochromic touch screens. *ACS Nano* 2017;11:4346–57.
- Grimsdale AC, Chan KL, Martin RE, Jokisz PG, Holmes AB. Synthesis of light-emitting conjugated polymers for applications in electroluminescent devices. *Chem Rev* 2009;109:897–1091.
- Ostroverkhova O. Organic optoelectronic materials: mechanisms and applications. *Chem Rev* 2016;116:13279–412.
- Lee C, Zaen R, Park KM, Lee KH, Lee JY, Kang Y. Blue phosphorescent platinum complexes based on tetradentate bipyridine ligands and their application to organic light-emitting diodes (OLEDs). *Organometallics* 2018;37:4639–47.
- Adamovich V, Boudreaux PLT, Esteruelas MA, Gómez-Bautista D, López AM, Onate E, et al. Preparation via a NHC dimer complex, photophysical properties, and device performance of heteroleptic bis(tridentate) iridium(III) emitters. *Organometallics* 2019;38:2738–47.
- Chen Z, Wu D, Han X, Liang J, Yin J, Yu GA, et al. A novel fluorene-based gold(I) complex with aggregate fluorescence change: a single-component white light-emitting luminophore. *Chem Commun* 2014;50:11033–5.
- Dong Y, Zhu F, Chen Z, Yin J, Liu SH. Single-component gold(I)-containing highly white-emissive crystals based on a polymorph doping strategy. *Mater Chem Front* 2019;3:1866–71.
- Wang XY, Hu XY, Yang XF, Yin J, Chen Z, Liu SH. Excitation wavelength-dependent nearly pure white light-emitting crystals from a single gold(I)-containing complex. *Org Lett* 2019;21:9945–9.
- a Petrenko A, Leitonas K, Volyniuk D, Baryshnikov GV, Belyakov S, Minaev BF, et al. Benzosenophenylpyridine platinum complexes: green versus red phosphorescence towards hybrid OLEDs. *Dalton Trans* 2020;49:3393–7. b Tsai YT, Raffay G, Liu HF, Peng BJ, Tseng KP, Hirsch L, et al. Incorporation of narcissistic self-sorting supramolecular interactions for the spontaneous fabrication of multiple-color solid-state materials for OLED applications. *Mater Chem Front* 2020; 4:845–50.
- Jayabharathi J, Anudeebhana J, Thankachalam V, Sivaraj S. Efficient fluorescent OLEDs based on assistant acceptor modulated HLCT emissive state for enhancing singlet exciton utilization. *RSC Adv* 2020;10:8866–79.
- Siddiqui QT, Awasthi AA, Bhui P, Parab P, Muneer M, Bose S, et al. TADF and exciplex emission in a xanthone-carbazole derivative and tuning of its electroluminescence with applied voltage. *RSC Adv* 2019;9:40248–54.
- Poriel C, Sicard L, Rault-Berthelot J. New generations of spirofluorene regioisomers for organic electronics: tuning electronic properties with the substitution pattern. *Chem Commun* 2019;55:14238–54.
- Ma H, Shen K, Wu Y, Xia F, Yu F, Sun Z, et al. High-color-purity and efficient solution-processable blue phosphorescent light-emitting diodes with Pt(II) complexes featuring $^3\pi\pi^*$ transitions. *Mater Chem Front* 2019;3:2448–54.
- Chai D, Zeng X, Su X, Zhou C, Zou Y, Zhong C, et al. A simple and effective strategy to lock the quasi-equatorial conformation of acridine by H-H repulsion for highly efficient thermally activated delayed fluorescence emitters. *Chem Commun* 2020; 56:2308–11.
- Shen Y, Xue P, Liu J, Ding J, Sun J, Lu R. High-contrast mechanofluorochromism and acidochromism of D- π -A type quinoline derivatives. *Dyes Pigments* 2019;163: 71–7.
- Chen Z, Nie Y, Liu SH. Fluorene-based mononuclear gold(I) complexes: the effect of alkyl chain, aggregation-induced emission (AIE) and mechanochromism characteristics. *RSC Adv* 2016;6:73933–8.
- Chen Z, Liu G, Pu S, Liu SH. Carbazole-based aggregation-induced emission (AIE)-active gold(I) complex: persistent room-temperature phosphorescence, reversible mechanochromism and vapochromism characteristics. *Dyes Pigments* 2017;143: 409–15.
- Chen Z, Liu G, Pu S, Liu SH. Bipyridine-based aggregation-induced phosphorescent emission (AIE)-active gold(I) complex with reversible phosphorescent mechanochromism and self-assembly characteristics. *Dyes Pigments* 2018;152: 54–9.
- Chen Z, Liu G, Pu S, Liu SH. Triphenylamine, carbazole or tetraphenylethylene-based gold(I) complexes: tunable solid-state room-temperature phosphorescence and various mechanochromic luminescence characteristics. *Dyes Pigments* 2018; 159:499–505.
- Tan S, Yin Y, Chen W, Chen Z, Tian W, Pu S. Carbazole-based highly solid-state emissive fluorene derivatives with various mechanochromic fluorescence characteristics. *Dyes Pigments* 2020;177:108302.
- Chen Y, Xu C, Xu B, Mao Z, Li JA, Yang Z, et al. Chirality-activated mechanoluminescence from aggregation-induced emission enantiomers with high contrast mechanochromism and force-induced delayed fluorescence. *Mater Chem Front* 2019;3:1800–6.
- Ikeya M, Katada G, Ito S. Tunable mechanochromic luminescence of 2-alkyl-4-(pyren-1-yl)thiophenes: controlling the self-recovering properties and the range of chromism. *Chem Commun* 2019;55:12296–9.
- Panda MK, Ravi N, Asha P, Prakasham AP. High contrast mechanochromic and thermochromic luminescence switching by a deep red emitting organic crystal. *CrystEngComm* 2018;20:6046–53.
- Tian H, Wang P, Liu J, Duan Y, Dong YQ. Construction of a tetraphenylethene derivative exhibiting high contrast and multicolored emission switching. *J Mater Chem C* 2017;5:12785–91.
- Hu J, Jiang B, Gong Y, Liu Y, He G, Yuan WZ, et al. A novel triphenylacrylonitrile based AIEgen for high contrast mechanochromism and bicolor electroluminescence. *RSC Adv* 2018;8:710–6.
- Zhu Yy, Xia Hy, Yao Lf, Huang Dp, Song Jy, He Hf, et al. High-contrast mechanochromic benzothiadiazole derivatives based on a triphenylamine or a carbazole unit. *RSC Adv* 2019;9:7176–80.
- He Hf, Shao Xt, Deng Ll, Zhou Jx, Zhu Yy, Xia Hy, et al. Triphenylamine or carbazole-based benzothiadiazole luminophors with remarkable solvatochromism and different mechanofluorochromic behaviors. *Tetrahedron Lett* 2019;60:150968.
- Mei J, Leung NLC, Kwok RTK, Lam JWY, Tang BZ. Aggregation-induced emission: together we shine, united we soar! *Chem Rev* 2015;115:11718–940.
- Luo J, Xie Z, Lam JWY, Cheng L, Chen H, Qiu C, et al. Aggregation-induced emission of 1-methyl-1,2,3,4,5-pentaphenylsilole. *Chem Commun* 2001:1740–1.
- Chi Z, Zhang X, Xu B, Zhou X, Ma C, Zhang Y, et al. Recent advances in organic mechanofluorochromic materials. *Chem Soc Rev* 2012;41:3878–96.
- Feng HT, Yuan YX, Xiong JB, Zheng YS, Tang BZ. Macrocycles and cages based on tetraphenylethylene with aggregation-induced emission effect. *Chem Soc Rev* 2018;47:7452–76.

- [46] Zhao J, Chi Z, Yang Z, Mao Z, Zhang Y, Ubba E, et al. Recent progress in the mechanofluorochromism of distyrylanthracene derivatives with aggregation-induced emission. *Mater Chem Front* 2018;2:1595–608.
- [47] Hong Y, Lam JWY, Tang BZ. Aggregation-induced emission. *Chem Soc Rev* 2011;40:5361–88.
- [48] Tang A, Chen Z, Liu G, Pu S. 1,8-Naphthalimide-based highly emissive luminogen with reversible mechanofluorochromism and good cell imaging characteristics. *Tetrahedron Lett* 2018;59:3600–4.
- [49] Gu J, Xu Z, Ma D, Qin A, Tang BZ. Aggregation-induced emission polymers for high performance PLEDs with low efficiency roll-off. *Mater Chem Front* 2020;4:1206–11.
- [50] Costa JCS, Lima MAL, Mendes A, Santos LMNBF. The impact of phenyl-phenyl linkage on the thermodynamic, optical and morphological behavior of carbazol derivatives. *RSC Adv* 2020;10:11766–76.
- [51] Wu Y, Jin P, Gu K, Shi C, Guo Z, Yu ZQ, et al. Broadening AIEgen application: rapid and portable sensing of foodstuff hazards in deep-frying oil. *Chem Commun* 2019;55:4087–90.
- [52] Cremer J, Briehn CA. Novel highly fluorescent triphenylamine-based oligothiophenes. *Chem Mater* 2007;19:4155–65.
- [53] Jiang Z, Chen Y, Yang C, Cao Y, Tao Y, Qin J, et al. A fully diarylmethylene-bridged triphenylamine derivative as novel host for highly efficient green phosphorescent OLEDs. *Org Lett* 2009;11:1503–6.
- [54] Venkateswararao A, Thomas KRJ, Lee CP, Li CT, Ho KC. Organic dyes containing carbazole as donor and π -linker: optical, electrochemical, and photovoltaic properties. *ACS Appl Mater Interfaces* 2014;6:2528–39.
- [55] Zhan Y, Yang Z, Tan J, Qiu Z, Mao Y, He J, et al. Synthesis, aggregation-induced emission (AIE) and electroluminescence of carbazole-benzoyl substituted tetraphenylethylene derivatives. *Dyes Pigments* 2020;173:107898.
- [56] Wei J, Liang B, Cheng X, Zhang Z, Zhang H, Wang Y. High-contrast and reversible mechanochromic luminescence of a D- π -A compound with a twisted molecular conformation. *RSC Adv* 2015;5:71903–10.
- [57] Shen XY, Wang YJ, Zhao E, Yuan WZ, Liu Y, Lu P, et al. Effects of substitution with donor-acceptor groups on the properties of tetraphenylethylene trimer: aggregation-induced emission, solvatochromism, and mechanochromism. *J Phys Chem C* 2013;117:7334–47.
- [58] Ye F, Liu Y, Chen J, Liu SH, Zhao W, Yin J. Tetraphenylene-coated near-infrared benzoselenodiazole dye: AIE behavior, mechanochromism, and bioimaging. *Org Lett* 2019;21:7213–7.
- [59] Bezikonnyi O, Gudeika D, Volyniuk D, Rutkis M, Grazulevicius JV. Diphenylsulfone-based hosts for electroluminescent devices: effect of donor substituents. *Dyes Pigments* 2020;175:108104.
- [60] Gudeika D, Lee JH, Lee PH, Chen CH, Chiu TL, Baryshnikov GV, et al. Flexible diphenylsulfone versus rigid dibenzothiophene-dioxide as acceptor moieties in donor-acceptor-donor TADF emitters for highly efficient OLEDs. *Org Electron* 2020;83:105733.
- [61] Danyliv Y, Volyniuk D, Bezikonnyi O, Hladka I, Ivaniuk K, Helzhynskyy I, et al. Through-space charge transfer in luminophore based on phenyl-linked carbazole- and phthalimide moieties utilized in cyan-emitting OLEDs. *Dyes Pigments* 2020;172:107833.